Chapter 10
Biomechanical Properties of the Trabecular Meshwork in Aqueous Humor Outflow Resistance

VijayKrishna Raghunathan

Introduction

Primary open angle glaucoma (POAG), age associated macular degeneration (AMD), and cataract are the three most common age associated ocular disorders worldwide, leading to vision loss. Among these vision loss in POAG and AMD are irreversible. The etiology and progression of these diseases are multifactorial [1, 2] although fibrosis, oxidative and senescence have been thought to be significant contributing factors. A key facet of fibrosis is a dynamic change in the extracellular matrix leading the tissue to become stiffer. The context in which this 'stiffness' is measured is dependent on the type of tissue, sample preparation, or the method by which it was measured. Regardless, a change in the biomechanical property of a tissue has profound implications on how cells respond to changes in their microenvironment. This is indeed true of the trabecular meshwork as well. Responsible for drainage of approximately 80% of the aqueous humor of the eye, dysfunction in the TM is thought to be the primary site of resistance, and lowering the intraocular pressure is the only modifiable risk factor in glaucoma, a major cause of irreversible blindness in the aging population [3–9]. The increased resistance to aqueous humor in POAG is thought to be due to dependent on a number of factors—senescence, matrix composition/morphology/mechanics, loss of intra- and inter-cellular pores, deposition of plaque like material, changes in segmental regions, loss of cells, and/or collapsing of the beams. With age, accumulation of extracellular matrix,

V. Raghunathan (✉)
The Ocular Surface Institute, University of Houston, Houston, TX, USA

Department of Basic Sciences, College of Optometry, University of Houston, Houston, TX, USA

Department of Biomedical Engineering, Cullen College of Engineering, University of Houston, Houston, TX, USA
e-mail: vraghunathan@uh.edu

I. Pallikaris et al. (eds.), *Ocular Rigidity, Biomechanics and Hydrodynamics of the Eye*, https://doi.org/10.1007/978-3-030-64422-2_10

thickening of the beams, and loss of TM cells have all been documented [10–14]. Lutjen-Drecoll et al. [15] demonstrated that with age the elastic fibers of the TM thicken with minimal changes to the elastin containing central core. Classical studies by Tripathi [16, 17] have shown elevated amounts of matrix proteins in the TM that were postulated to contribute to increased resistance to outflow. Data emanating from studies over the past 4 decades are yet to identify the molecular mechanisms or the implications of mechanical changes in the TM contributing to the etiology and progression of glaucoma. Such increase in thickness may contribute to the changing biomechanics in glaucoma or age, and this is yet to be demonstrated.

The Importance of Studying Biomechanics of the Outflow Pathway

The anterior segment of the eye is complex and includes the cornea, lens, iris, ciliary body, trabecular meshwork (TM) and Schlemm's canal (SC). The TM and SC are located at the iridocorneal angle and primarily regulate and drive the drainage of aqueous humor. The TM is an incredibly complex structure (Fig. 10.1) comprised primarily of three regions which differ in both structure and function [18–22]. Anterior to posterior, first is the <20 μm thin juxtracanalicular (JCT) or cribiform region (primary site of resistance to outflow) that is separated from the endothelial cells of inner wall of the Schlemm's canal via a discontinuous basement membrane. The JCT is a made of 2–5 layers of cells embedded in a wide variety of macromolecules and residing over loose fibrillar ECM. This is followed by the corneo-scleral trabecular meshwork (CTM) comprised of thick 8–15 trabecular beams/lamellae made of Col I/III, and elastic fibers. Each layer is covered by cells on a basal lamina rich in laminin and Col IV. Posteriorly, this is followed by 1–3 layers of uveal trabecular meshwork (UTM) whose lamellae are thinner than those observed in the CTM. These together form a sponge-like filter whose porosity varies between and within the three layers.

Approximately 75% of all aqueous humor flows through the TM and SC [23, 24]. The inner wall cells are currently thought to contribute only about 10% of the total resistance [25]. Since the cells in the JCT of the meshwork are not continuous, the bulk of outflow resistance would lie with the extracellular matrix (ECM) of the meshwork at the JCT. ECM components include fibrillar scaffolding proteins (e.g. fibronectin, laminin, collagen etc), non-structural matricellular proteins (e.g. SPARC, matrix gla protein, periostin, CCN family of proteins, thrombospondin, tenascin etc), and glycosylated proteoglycans. Common proteoglycans observed in the TM are glycosaminoglycans [(chondroitin sulfate, heparan sulfate, hyaluronan etc), and versican, perlecan, decorin, biglycan etc]. These together provide structural and mechanical properties to the tissue and adequate surface for the attachment of cells and by acting as load bearing structures. Further, through the presentation of various ligands, ECM components can bind, sequester, and stabilize signaling molecules to modulate essential cellular processes such as migration, proliferation, differentiation, and cell fate determination.

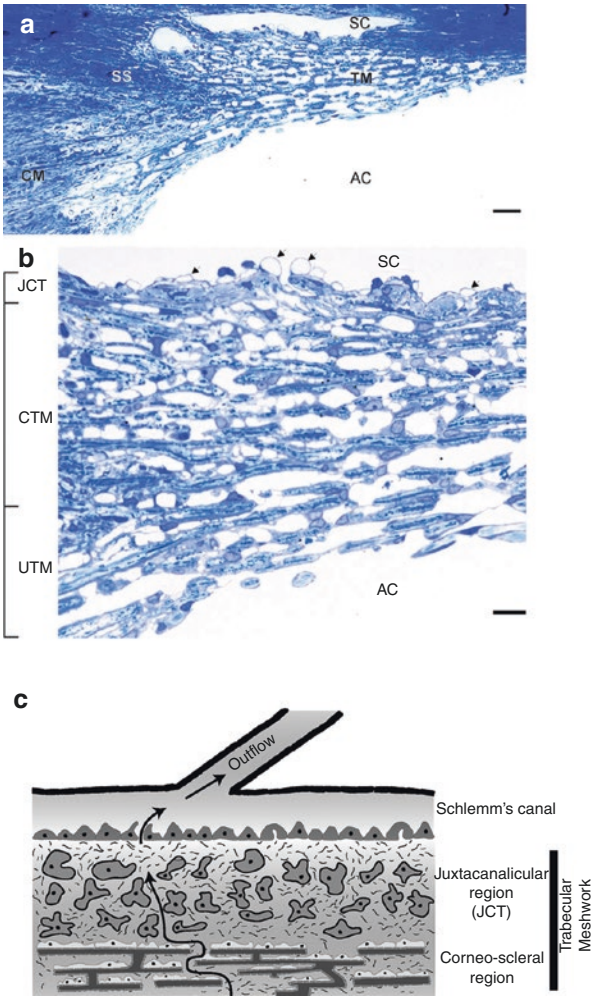

Fig. 10.1 The trabecular meshwork: (**a**) Shows a view of the trabecular meshwork that separates the aqueous humor in the anterior chamber from the canal of Schlemm. *TM* trabecular meshwork; *SC* Schlemm's canal; *AC* anterior chamber; *SS* scleral spur; *CM* ciliary muscle. Magnification bar is 20 μm. (**b**) A magnification of the trabecular meshwork demonstrating the 3 regions: *UTM* uveal trabecular meshwork; *CTM* corneoscleral trabecular meshwork; *JCT* Juxtacanalicular tissue. Magnification bar is 5 μm. (**c**) Schematic illustrates the direction of outflow across the trabecular meshwork. (**a**, **b**) are reproduced with permission from Tamm [18]

For any tissue, the intimate interaction between cells and their matrix contribute to the mechanical properties. The contribution of either component in defining these properties are quite difficult to isolate. Biomechanical stimuli—such as mechanical stretch, pulsatile motion, compression, shear, pressure, static cell guidance cues etc. are all integral components of the cellular microenvironment in the tissue. That cells are sensitive to dynamic mechanical forces such as shear stress, pressure, and stretch

are well recognized [26, 27]. Nevertheless, a plethora of passive biophysical tissue attributes of tissue exists such as stiffness or nanotopography alter cellular proliferation, migration, expression, and differentiation [28–32]. Whilst these cues may appear to be passive at a given instant, they are capable of changing with time, stimulus, and/or intervention. Over the past decade a number of groups have demonstrated the impact that biophysical stimuli on tissue homeostasis, development, differentiation and disease. It is therefore paramount to place these in the context of tissue function. Biophysical, biochemical, and genetic factors act in concert to dynamically govern the continuous interactions between cells and their extracellular microenvironment. Using other cell systems it was shown that cells cultured on stiffer substrates adopt a more contractile tone [33–36]. Truly, TM cells have been reported to be contractile [37, 38], and this is thought to contribute to matrix changes observed in the tissue in POAG leading to outflow resistance [39–41]. Congruently, the importance of Rho signaling and its effect on lowering IOP has been the target for development of novel drugs targeting the conventional outflow pathway [42–44].

Despite the demonstrated importance of biophysics on cellular behaviors, and its potential to mediate IOP, the complexity of the outflow tract has prevented its complete mechanical characterization. Nearly a decade ago, Overby et al. [45] proposed a paradigm where the JCT and inner wall endothelial cells synergistically control outflow resistance. Emerging data in the field document that the resistance goes beyond the Schlemm's canal by demonstrating a dynamic range in resistance to aqueous outflow by the distal vessels of the conventional outflow pathway when the TM was excised ex vivo [46]. Thus, a full characterization of mechanical properties is essential to account for the substantial heterogeneity and anisotropic organization of the tissues involved, as well as how these properties change in disease. It would be wise to note that there are no determined standards that exist to define mechanical properties of ocular tissues. Despite these challenges, a number of laboratories have made significant inroads in characterizing the material properties using various techniques and determining how these properties may influence cell behavior and outflow function. In this chapter we shall explore further the published data, and relevance of biomechanics to TM mechanobiology and outflow resistance. Data pertaining to the Schlemm's canal are not discussed here.

Parameters Defining the Mechanical Properties of Biological Materials

Biological materials such as tissues are difficult to define due to the complex nature of their compositions: ECM, cells, soluble factors, and interstitial fluid. The trabecular meshwork is unique in the sense that it potentially has both *isotropic* (direction independent) and *anisotropic* (direction dependent) characteristics. The way the collagen lamellae are organized around the circumference is highly aligned while the loosely packed matrix of the JCT is stochastic in organization. Further, judging by the anatomical organization of the TM, it is *inhomogeneous in toto*

although there may be certain localized regions where the material may be considered *homogeneous*. For example, flow across the TM has been recognized to be segmental i.e. there are regions of high, low, and medium flow with marked differences in the expression of select matrix/matricellular proteins [47–53]. However, whether there are intrinsic structural changes between these segments, and if these vary with time, stimulus, disease are unknown. As such, cells aligned with the collagen fibers may experience 'contact guidance' and experience *static* stretch. It is been postulated that the aqueous system behaves like a mechanical pump [54, 55] to produce *cyclical* strain that is capable of transferring cyclical stretch and compression to the tissue/cells/ECM. Thus the forces experienced by cells are both tangential and perpendicular to their alignment on matrix fibers/bundles. Combined with a possible pulsatile motion, the tissue (cells & matrix) potentially thus experience localized and bulk tensile and compressive loading. Such a property that defines the negative of the ratio of transverse strain to corresponding axial strain is defined as Poisson's ratio (ν) and is essentially constant for any given material. Isotropic materials have a Poisson's ratio between -1.0 and 0.5. The Poisson's ratio of most engineering materials is typically $0.2 < \nu < 0.5$, incompressible materials with elastic deformations will have $\nu = 0.5$, while $\nu = 0$ demonstrates that there is no change in transverse strain.

Combining all these attributes, the most commonly used term to define the mechanical property of a biological tissue in the ocular field is elastic modulus often referred to simply as 'stiffness'. It is a measure of the tendency of a material to resist deformation under stress (force applied per unit area). The ratio of stress to strain (change in deformation per original length) when load is applied in plane is defined as the Young's modulus. The term Young's modulus is true when a material's property is such that the relationship between stress and strain is linear. This is often not the case for biological materials where the modulus varies with the amount and rate of strain, and direction of loading. As such, tissue 'stiffness' is simply referred to as elastic modulus/apparent elastic modulus/tensile modulus etc. depending on the method used. That being said, measures of TM tissue stiffness cannot be taken as absolute unless the methods by which samples are prepared, instrumentation/techniques used, parameters applied for determination are all taken into consideration. Nonetheless values reported in literature provide information on the differences observed between homeostasis and disease to a reasonable extent.

Box 1 Definition of Basic Parameters

Elastic modulus: The modulus of elasticity or elastic modulus is the property of a material that defines how deformable it is under various loads applied. Elastic materials do not have a permanent irreversible change in structure and behavior when a load is applied. The factors that describe the relation between deformation and applied force are termed as 'elastic constants' and the modulus is just one such constant. In biological science research, stiffness and elastic modulus are often used interchangeable, and this has not been without

controversy. However, in engineering context, stiffness refers to the force-deformation relationship of the whole system, rather than an intrinsic property of the material. The most commonly used parameter to define the mechanical property of the trabecular meshwork is the elastic modulus, which is defined as Young's modulus. It must be noted that the Young's modulus usually refers to the modulus determined by tensile testing and is defined as follows: For an isotropic material, when a uniaxial tensile stress is applied, the initial slope, where a linear relationship exists between axial stress and axial strain, is defined as the tensile modulus of elasticity or Young's modulus (E) i.e. $E = \sigma/\varepsilon$ in units of N/m^2 or Pa. This linear relationship is also termed Hooke's law (Fig. 10.2).

Viscoelasticity: A number of materials have an elastic component and a viscous component whose stress-strain relationship depends on 'time'. It must be noted that viscoelastic materials will return to their original shape when the applied force is removed (elastic response) although with prolonged time (viscous response) this will not occur. (Figure 10.2 shows difference between elastic loading and viscoelastic loading also termed hysteresis). Cells and tissues have viscoelastic properties with small perturbations at a cell membrane eliciting an elastic response while larger forces eliminate this elastic response.

Reported Mechanical Characterization of the Trabecular Meshwork

Very few studies have actually evaluated the mechanical properties of trabecular meshwork either *in vitro* or *ex vivo*. The most common parameter reported is the elastic modulus; very little is known about the viscoelastic properties of the TM. These measurements have been made directly and indirectly using a number of techniques. To our knowledge, there are no studies that have reported any mechanical characterization of the TM tissue in vivo. Further, the effects of drugs used to lower IOP on TM biomechanics is largely lacking. However, recent studies combing imaging and computational methodologies hold great promise in accurately characterizing the TM.

Human

The trabecular meshwork, while under constant circumferential stress, is also subjected to compressive loading by dynamic remodeling of the extracellular matrix in addition to modulation in cellular cytoskeletal dynamics. Atomic force microscopy is an indentation technique used to determine the mechanical properties in a localized environment and is thus suitable method for TM. Less than a decade ago, the

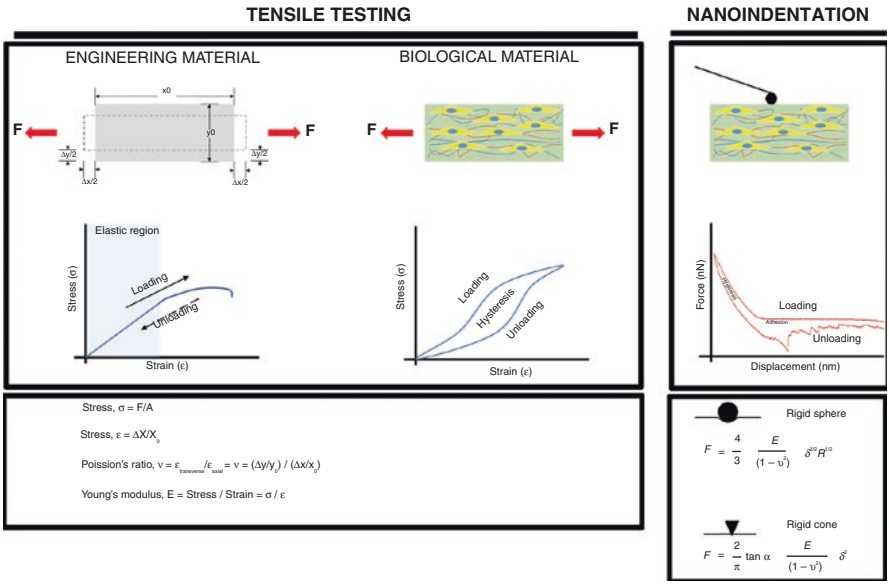

Fig. 10.2 Tensile testing vs nanoindentation. A comparison of uniaxial tensile behavior of engineering vs biological materials is illustrated. Biological materials are viscoelastic and exhibit hysteresis. Nanoindentation methods enable the determination of mechanical properties at a localized area rather than the bulk of the material. General equations governing the definition of elastic modulus are provided. *F* force; *E* elastic modulus; δ indentation; *R* radius of spherical indenter; α half angle of cone; *A* area; ν Poisson's ratio of material; ε strain; σ stress

elastic modulus of the human TM, at the JCT side, was quantified using AFM [56]. This study was particular important as it the first to report that the apparent elastic moduli of human TM isolated from glaucomatous donors was significantly greater (~20 fold at ~80 kPa) than from normal donors (~4 kPa). There has been skepticism with the manner in which the tissue was prepared and speculation that the cyanoacrylate glue used to adhere the sample may have resulted in an artifactually high value. However, in the same study the authors demonstrate a large range of values for the elastic modulus along the TM suggesting there may have some regional variations. More recently, Vranka et al. [53], using AFM, demonstrated that the elastic moduli of TM (JCT side) varied between the segmental flow regions with mean values for low flow (LF) regions at ~7 kPa vs ~3 kPa for high flow (HF) regions in normal TM obtained from 24 h ex vivo anterior segment perfusion cultures at 1x pressure. Further, they demonstrated that with elevated pressure (2×) for 24 h in normal tissues, HF regions became softer (~1.3 kPa) while LF regions appeared to become stiffer (~9.7 kPa). In a further recent follow up, Raghunathan et al. [57] demonstrate that glaucomatous LF tissues have a mean elastic modulus of ~75 kPa while glaucomatous HF tissues were ~2 kPa. These two recent studies did not use any glue as a mounting agent to adhere the TM tissue [58] and measured the JCT side. These values are in agreement with those reported by Last et al. [56] for

glaucomatous TM. In another study [59], using AFM, the elastic modulus of TM from normal eyes was ~1.37 kPa while that of glaucomatous eyes was ~2.75 kPa and observed no significant differences between HF or LF regions in either group; here, the TM was not excised from the corneo-scleral wedge, thus the measurements were likely performed away from the JCT and on the uveo/corneo-scleral side.

Using uni-axial tensile testing, the most commonly and traditionally used method to determine tissue mechanical property, the tensile modulus of human TM from both normal and glaucomatous donors has been reported. Camras et al. [60–62] reported that the Young's modulus of glaucomatous TM 51.5 MPa while that of non-glaucomatous tissues was 12.5 MPa. Additionally, Camras et al. [60] also noted substantial inhomogeneity, with variations in modulus in different segments within the TM, implying the meshwork may exhibit segmental mechanics suggestive of segmental outflow [49, 51, 63–66] although these were not investigated. Whilst these values appear to contradict the findings of Last et al. [56], it is imperative to understand that the methods used in the two studies are vastly different. Also, the organization of fibrillar structural components in tissues can exhibit substantial anisotropy, making tensile testing highly dependent on the orientation of the sample. All of these challenges are exemplified in the TM. Further, the elastic moduli values reported depends on **(i)** the applied stress/strain, **(ii)** the hydration state, **(iii)** time between tissue excision and measurement, **(iv)** alignment with the tissue grips, **(v)** temperature, **(vi)** storage and bathing medium, and **(vii)** precise location/anatomy of tissue tested [67–70]. Any method used to determine the mechanical property of soft tissues will have to simulate the native environment during testing. It is likely that the contribution of the corneo-scleral portion of the meshwork is greater with the tensile testing than that of JCT. Although, why the values reported for the TM are significantly larger than values reported for scleral biomechanics are unclear. A major factor with tensile measurements is the clamping force applied to hold the tissue. In the case of the TM measurements, it is unclear what these were or how they affect the moduli values reported. Also, tensile testing informs us of the bulk properties of tissue and do not account for the individual contribution of cells versus matrix components or the contribution from segmental regions.

Other methods have also been used to estimate the modulus of the TM, notably by combining optical coherence tomography (OCT) images and engineering models. Johnson et al. [71] estimated the elastic modulus of the TM to be 128 kPa using an analytical model of beam-bending under uniform load for a linearly elastic material with simplified geometry and based on changes in TM and SC thickness. Subsequently, using a nearly incompressible neo-Hookean solid model, Pant et al. [72] estimate the elastic modulus for TM as 5.75 kPa by inverse finite element modeling (FEM). In these above methods, the influence of TM compressibility was not taken into account, although the values estimated by Pant et al. [72] are closer to those reported using AFM by Last [56], Vranka [53], Raghunathan [57] and Wang et al. [59]. Values obtained from FEM and AFM must be compared only with caution since the methods in which the load is applied are quite different (tension in OCT imaging, vs compression in AFM). Interestingly, using inverse FEM, Wang et al. [59] estimated normal TM modulus at 70 ± 20 kPa and glaucomatous TM

modulus at 97 ± 19 kPa which is approximately 10–15 times greater than that estimated by Pant et al. [72]. A major difference between these two studies are in how the images were collected, analyzed, and thus used to create the mesh required for FEM. Further, a major factor contributing to the discrepancy in the values in these two studies is how the areas and thickness of Schlemm's canal were factored.

Non-human Primate

The structure of the eye's aqueous humor outflow system and its influence on IOP have been studied in humans and animals for many years and continue to be investigated. Of the available animal models, experimental glaucoma (ExGl) in the non-human primate (NHP), induced by subtotal laser photocoagulation of the trabecular meshwork (TM), is considered the most predictive for drug efficacy in the human [73]. Morphological and hydrodynamic data in this model suggest that fibrosis of the TM and adjacent inner wall of Schlemm's canal (SC) reduces the area for conventional aqueous outflow, leading to decreased outflow facility, and elevated IOP [74–78]. Furthermore, the classic arcuate mid-peripheral visual field losses observed in human patients with primary open angle glaucoma (POAG) and elevated IOP have also been observed in visual field testing of NHPs with ExGl [79]. Additional evidence suggests that aqueous humor flow in eyes with ExGl is largely diverted to the small unlasered area of TM, suggesting a capacity for this tissue to dynamically compensate both structurally and functionally, accommodating the increased flow [76]. However, very little is known about the mechanical properties of the NHP TM and if there is any relevance to glaucoma. To the best of our knowledge, there is only one study [80] that reports the elastic modulus in NHPs; mean elastic modulus as determined by AFM was 3.3 ± 0.32 kPa for control animals, while the unlasered regions of TM in ExGl NHPs were approximately 300 Pa (0.30 kPa). This data suggested dynamic compensation for chronic IOP elevation in ExGl and that a softer TM promotes increased outflow, provided by the capacity for unlasered primate TM cells in normal primate eyes to compensate for increased IOP and reduced overall outflow from the eye by altering the composition and subsequent mechanical properties of the matrix in the JCT region. However, a principal limitation of that investigation is the lack of knowledge as to the mechanism of action or class of the topical agents previously administered to these NHPs, as well as the need for sporadic to frequent treatment to manage excessively high IOP in eyes with ExGl.

Mice

Mice are extensively used to study pathophysiology of the TM due to their ease of genetic manipulation, ability to administer treatments, and similarity of the conventional outflow pathway with humans. However mechanical characterization of

rodent TM, although much sought after, has been quite challenging to perform, and as such only a couple of studies have reported the elastic modulus of the mouse TM using various methods. The first report was by Li et al. [81] combining spectral domain OCT images and mathematical modeling. They made the following assumptions for these measurements: that a decrease in Schlemm's canal lumen was by TM deformation, that there was change in the width of SC, that pressure inside SC lumen was independent of IOP, and that TM was linearly elastic. The elastic modulus was reported as 2.16 kPa in control eyes and 3.46 or 5.01 kPa in BMP2 overexpressing eyes (as a model for ocular hypertension) after 7 or 10 days respectively. It is important to note that the parameters used for mathematical modeling were identical for all mice across the groups, and thus differences in anatomical and pressure parameters between animals or regional variations were not considered.

More recently, Wang et al. [82] measured TM modulus in 10–20 μm thick sagittal cryosections after whole globe perfusions. They compared two freezing techniques one with a cryoprotectant (15% glycerol) and one without. In this initial study, the authors found no correlation between outflow facility and TM modulus in 5 eyes (C57BL/6J) whose TM were frozen with a cryoprotectant or in 11 eyes (CBA/J) whose TM were frozen without cryoprotectant. The elastic modulus of the TM in cryosections obtained with cryoprotectant was 3.22 ± 1.84 kPa while those without cryoprotectant was 3.84 ± 3.37 kPa. Segmental flow observations were not taken into account in this study. In a follow up study, Wang et al. [83] report that TM modulus from 18 C57BL/6J mice was 2.20 ± 1.12 kPa vs 3.08 ± 3.55 kPa in 10 CBA/J mice. Further, they demonstrated that TM modulus was 2.38 ± 1.31 kPa in mice treated with dexamethasone for 14 days vs 1.99 ± 0.91 kPa in vehicle control mice. For the first time, this study report a small but significant correlation between TM modulus and outflow resistance but not IOP with dexamethasone treatment using two strains (C57BL/6J and CBA/J) of mice. This is especially important considering mechanical properties were first suggested to impact the resistance to aqueous outflow. Although rehydrated frozen sections have been used for AFM but non-ocular investigators, this is not without limitation. Whether such freeze-thaw cycles alters GAG content that contribute to tissue compression resistance were not reported or discussed.

Rabbit

Using AFM, we reported that the elastic modulus of the TM (JCT side) in adult New Zealand white rabbits as 1.03 ± 0.55 kPa and that its modulus was elevated threefold to 3.89 ± 2.55 kPa with 3 weeks of 0.1% (w/v) topical dexamethasone treatment in vivo. In our study irrespective of any measured change in IOP, a change in the mechanical property of the TM was observed. Long-term consequences of steroid administration on IOP changes or TM biomechanics in rabbits were not determined, although steroid induced IOP elevation in humans and mice have been reported [84, 85].

Rat

Huang et al. [86] report a method of estimating the elastic modulus of the TM in rat eyes. This involved perfusion of the eyes with Evans blue (a non-specific tracer to the TM), flat mounting the anterior segments, subsequently measuring indentation on the uveal side of the TM by AFM to estimate elastic modulus, and finally using the indentation values with a mathematical model for non-Hookean materials to verify the moduli measurements. The geometric mean elastic modulus of the TM was reported as 162 ± 1.2 Pa.

Porcine

Elastic modulus of the porcine TM has been evaluated both by AFM and tensile testing. Camras et al. [60, 62] reported the tensile elastic modulus of porcine TM as 2.49 MPa, while Yuan et al. [87] reported the indentation modulus by AFM as 1.38 kPa.

Considerations While Interpreting AFM Moduli Measurements

Sample preparation: Preparation of biological samples is crucial in biomechanical characterization. One of the major advantages of using AFM is that the tissue needn't be fixed or dehydrated and can be characterized in a biomimetic environment without the need for fixation or dehydration. The most common method to immobilize biological samples is by using cyanoacrylate or fibrin based glues that can potentially introduce artifacts [88, 89]. For very small samples, Cell-Tak or poly-L-lysine may be used. While minimizing the amount glue to minimize errors or discarding artifactual data are feasible, it is preferred that sample preparation is objective and controlled. This problem is increasingly being recognized and glue-free methods are being developed [58, 90]. Similarly, avoiding freeze-thaw of tissues to prevent alterations in tissue composition should be preferred.

Anatomical location: This is undoubtedly an important consideration while performing AFM on TM. The TM is defined by 3 major regions: uveo-scleral meshwork, corneo-scleral meshwork, JCT and cribiform plexus. Thus whether measurements are performed on the JCT side or the uveal-/corneo-scleral side is critical. Further, how the cells differ in each region and what their contribution to mechanics is poorly defined. Depending on the region of the TM, cells may either form sheets covering ECM structures or they may be scattered throughout the ECM forming occasional gap and adherens junctions. Elastic fibers in the TM have a circumferential alignment, yet the JCT is loosely organized with large open spaces.

Segmental flow regions of the TM also ought to be considered while performing experiments.

Hydration medium: Tissues are hydrated in vivo and thus have to be adequately and appropriately hydrated while performing AFM. Physiological buffer like phosphate buffered saline or Hank's balanced salt solution with divalent salts (Ca^{2+}/Mg^{2+}) will minimize electrostatic interactions and osmotic pressure, and prevent potential swelling artifacts.

Cantilever considerations: Since AFM is dependent on deflection of a cantilever; the choice of appropriate cantilever stiffness (spring constant) should be matched with the sample stiffness. i.e. if a stiff cantilever is used to measure a sample softer by orders of magnitude, large deformations would not lead to detectable cantilever deflection. At the same time, the spring constant cannot be too small such that drag force due to motion through the buffer generates appreciable deflection. Further, the osmolarity and viscosity of the medium being used to perform the measurements are important to consider as they can influence cantilever deflection. In addition, prior to every experiment, it is important to calibrate the spring constant and optical sensitivity of the cantilever. For all samples, optimal parameters for approach velocity and indentation depth have to be kept consistent. When using elastic approximations for viscoelastic tissues, approach velocity of the cantilever must be carefully controlled.

Indenter shape and depth: This is a critical factor while obtaining force versus indentation curves for AFM analysis. The models used to fit force versus indentation curves are geometry specific: rigid cone, sphere, or flat cylinder [91, 92]. If cantilevers are modified with a sphere, the diameter of the sphere factors heavily in indentation depth and subsequent analysis of elastic modulus [93–96]. For thin samples such as tissues or cell derived matrices, it is essential to consider the influence of the underlying substrate, which is typically far stiffer. To mitigate substrate effects the general rule is to limit the indentation depth to approximately 10% of the total sample thickness [97, 98]. Further, due to the viscoelastic nature of biological tissues, the velocity of indentation is critical while performing measurements.

A Brief Glimpse on the Cellular Consequences or Mechanobiology of the Trabecular Meshwork

Besides using genetic or ocular hypertension models by steroid administration, most of our understanding of TM biology including the study of cell signaling pathways come from traditional cell culture of primary human TM cells isolated from whole eye globes or corneo-scleral rims on rigid non-physiological polystyrene/tissue culture plastic (TCP) or glass bottom dishes. These surfaces have elastic moduli of the order of >1 GPa which is several orders of magnitude greater than what TM cells sense in the native environment, are generally topographically flat compared to a topographic rich ECM in vivo, chemically devoid of functional heterogeneity unlike the TM tissue. An overwhelmingly large body of literature document

the biology of cells are vastly different when presented with relevant substratum biophysical properties (stiffness, topography, chemical and physical heterogeneity, porosity) in vitro [99, 100]. It is thus evident that TCP dishes do not provide the necessary cues that may be essential to dictate cell fate.

Considering just one factor, substrate rigidity, a number of studies have demonstrated that TM cells respond differentially in the presence or absence of a number of soluble factors when cultured on hydrogels of biomimetic elastic modulus. For example, Schlunck et al. [101] demonstrated that cell spreading and focal adhesion size, FAK activation, serum-induced ERK phosphorylation, expression and recruitment of αSMA to stress fibers and all increased with substrate rigidity. They further demonstrated that the morphology of fibronectin deposits differed on the various matrices. Interestingly, elevated amounts of myociling and αB-crystallin were observed on softer gels. Subsequently, Han et al. [102] further showed that with increasing substratum rigidity and TGFβstimulus, protein expression (collagen VI, αSMA, fibronectin etc) similar to that reported in primary open-angle glaucoma was observed and partially mediated via non-Smad signaling (ERK, AKT, or PI3K). We previously showed that an increase in substrate stiffness increases secreted frizzled related protein 1 (SFRP1, a potent antagonist of the Wnt pathway [103]) expression level in HTM cells [104]. SFRP increases with senescence, with steroid treatment in HTM cells, and can actually increase senescence in these cells [105]. Using glass/plastic surfaces increases in TM cell stiffness have been observed with dexamethasone treatment, Wnt inhibition (both canonical and non-canonical), or with replicative senescence [106–108]. The modulatory effects of Wnt signaling in cells cultured on substrates of varying rigidity are yet to be evaluated.

In other studies, Wood et al. [109], Thomasy et al. [110, 111] demonstrate that substratum rigidity modulates TM cell response to actin disruption (by Latrunculin-B) partially via mechanotransducers YAP and YAZ. Cells on softer substrates demonstrated lower cell proliferation and attachment. Further data from these studies demonstrated that TM cells cultured on hydrogels of normal or glaucomatous tissue stiffness responded differently to Latrunculin-B treatment in comparison with when cultured on TCP; notably decreases in ECM protein expression, and lower cellular responses to mechanotransducers when treated with Lat-B were observed on softer gels. McKee et al. [112] demonstrated that primary HTM cells adhered to stiffer substrates were significantly more responsive to Lat-B suggesting that the effects of Lat-B treatment would be most pronounced in glaucomatous eyes with a stiffer HTM. They also show a rebound effect on HTM cell stiffness as the actin cytoskeleton was reforming after the Lat-B treatment. Considering a number of cytoskeletal modulators are in clinical trial for IOP reduction, there is a possibility that a number of drugs may be inadvertently considered ineffective because pre-clinical tests were performed on irrelevant substrates.

Other biomechanical stimuli such as stretch (due to anisotropy of the ECM, or dynamic strain due to pulsatile motion) also have profound effects on TM cell behaviors. Static stretch, due to anisotropy of or underlying substrates, was sufficient to increase myocilin and versican expression in TM cells in a size dependent manner [113]. Non-topographic static stretch was shown to elevate aquaporin-1

levels and inversely correlated with lactate dehydrogenase release suggesting a possible role in cytoprotection [114]. From non-ocular systems it is evident that both cyclic and static strain modulate mechanosensors (integrins and focal adhesion complexes) differentially to effect a plethora a signaling cascades downstream. Similarly, in the context of TM cell culture in vitro, dynamic stretch elicited by cyclic strain has been shown to affect a myriad of cellular function and gene/protein expression. Again, not all genes/proteins are modulated in a similar or expected manner. Cyclic stain, on the other hand, has been shown to alter the actin cytoskeleton, transiently decrease αB-crystallin, significantly increase both secretion and transcription of IL-6, elevated production of metalloproteinase-2 (MMP-2), MMP-14 and tissue inhibitor of metalloproteinase-1 (TIMP-1) but not MMP9 or TIMP-2, increased extracellular secretion of ATP and adenosine, increased phosphorylation of protein kinase B, elevated expression of vertebrate lonesome kinase, secretion of autotaxin, and modulate mTOR signaling/autophagy to name a few [115–126]. Such phenomena are not unique to the TM and are prevalent in almost every tissue/disease model. Whether substratum stiffness plays a role in stretch mediated cellular outcomes remains to be seen. Despite all these, studies are continued to be performed on 2D surfaces with artificial chemistry. In an attempt to move towards a biomimetic approach, our lab and others have begun to move towards the use of 3D scaffolds or cell derived matrices to evaluate TM behavior [57, 108, 127–129]. Such models have been used to both evaluate the effects of drugs [129] or to simply demonstrate that pathologic matrices are capable to driving healthy cells towards a glaucomatous phenotype [57].

Summary

The overview presented here is by no means exhaustive, but is meant to demonstrate the complexities and differences in quantifying TM mechanics and how it influences their biology. Changes in mechanics by themselves are insufficient to understand the fundamental question: what drives outflow resistance and how this regulates subsequent elevated intraocular pressure? It would appear from the existing knowledge that a better means to integrate the biomechanics with the cell biology concurrent with sophisticated tools to dissect the signal transduction pathways as it pertains to cytoskeleton/ECM/tissue remodeling would be ideal. Recent advances in multi-photon microscopy and second harmonic imaging capabilities are capable of providing high resolution spatial distribution of cellular and extracellular structures and proteins. Particularly, they are useful to resolve the associations between tissue architecture, cells and ECM proteins [130–132]. In addition to static imaging, dynamic motion of the TM has recently been imaged by phase-sensitive optical coherence tomography [55] allowing for live visualization of TM in vivo. When all the data from various techniques are integrated, they can then be used for predictive mathematical modeling in silico. Computational modeling of TM behavior will provide valuable information to predict the effects of drugs that alter

aqueous humor drainage and regulation of IOP restricting the number of animal studies that may be required for drug development.

References

1. Seddon JM. Genetic and environmental underpinnings to age-related ocular diseases. Invest Ophthalmol Vis Sci. 2013;54:ORSF28–30. https://doi.org/10.1167/iovs.13-13234.
2. Chew EY. Nutrition effects on ocular diseases in the aging eye. Invest Ophthalmol Vis Sci. 2013;54:ORSF42–7. https://doi.org/10.1167/iovs13-12914.
3. Quigley HA. Open-angle glaucoma. N Engl J Med. 1993;328:1097–106. https://doi.org/10.1056/NEJM199304153281507.
4. Johnson M. What controls aqueous humour outflow resistance? Exp Eye Res. 2006;82:545–57. https://doi.org/10.1016/j.exer.2005.10.011.
5. Gottanka J, Johnson DH, Martus P, Lutjen-Drecoll E. Severity of optic nerve damage in eyes with POAG is correlated with changes in the trabecular meshwork. J Glaucoma. 1997;6:123–32.
6. Lutjen-Drecoll E. Morphological changes in glaucomatous eyes and the role of TGFbeta2 for the pathogenesis of the disease. Exp Eye Res. 2005;81:1–4. https://doi.org/10.1016/j.exer.2005.02.008.
7. Rohen JW, Lutjen-Drecoll E, Flugel C, Meyer M, Grierson I. Ultrastructure of the trabecular meshwork in untreated cases of primary open-angle glaucoma (POAG). Exp Eye Res. 1993;56:683–92.
8. Quigley HA, Broman AT. The number of people with glaucoma worldwide in 2010 and 2020. Br J Ophthalmol. 2006;90:262–7. https://doi.org/10.1136/bjo.2005.081224.
9. Klein R, Klein BE. The prevalence of age-related eye diseases and visual impairment in aging: current estimates. Invest Ophthalmol Vis Sci. 2013;54:ORSF5–ORSF13. https://doi.org/10.1167/iovs.13-12789.
10. Alvarado J, Murphy C, Polansky J, Juster R. Age-related changes in trabecular meshwork cellularity. Invest Ophthalmol Vis Sci. 1981;21:714–27.
11. Alvarado J. Presence of matrix vesicles in the trabecular meshwork of glaucomatous eyes. Graefes Arch Clin Exp Ophthalmol. 1982;218:171–6.
12. Alvarado J, Murphy C, Juster R. Trabecular meshwork cellularity in primary open-angle glaucoma and nonglaucomatous normals. Ophthalmology. 1984;91:564–79. https://doi.org/10.1016/S0161-6420(84)34248-8.
13. Miyazaki M, Segawa K, Urakawa Y. Age-related changes in the trabecular meshwork of the normal human eye. Jpn J Ophthalmol. 1987;31:558–69.
14. McMenamin PG, Lee WR, Aitken DA. Age-related changes in the human outflow apparatus. Ophthalmology. 1986;93:194–209.
15. Lütjen-Drecoll E, Rohen JW. Morphology of aqueous outflow pathways in normal and glaucomatous eyes. In: Ritch R, Shields MB, Krupin T, editors. The glaucomas. St. Louis: Mosby; 1996. p. 89–123.
16. Tripathi RC. Pathologic anatomy of the outflow pathway of aqueous humour in chronic simple glaucoma. Exp Eye Res. 1977;25:403–7. https://doi.org/10.1016/S0014-4835(77)80035-3.
17. Tripathi RC, Tripathi BJ. Contractile protein alteration in trabecular endothelium in primary open-angle glaucoma. Exp Eye Res. 1980;31:721–4. https://doi.org/10.1016/S0014-4835(80)80056-X.
18. Tamm ER. The trabecular meshwork outflow pathways: structural and functional aspects. Exp Eye Res. 2009;88:648–55. https://doi.org/10.1016/j.exer.2009.02.007.
19. Lütjen-Drecoll E. Functional morphology of the trabecular meshwork in primate eyes. Prog Retina Eye Res. 1999;18:91–119. https://doi.org/10.1016/S1350-9462(98)00011-1.

20. Lütjen-Drecoll E, Schenholm M, Tamm E, Tengblad A. Visualization of hyaluronic acid in the anterior segment of rabbit and monkey eyes. Exp Eye Res. 1990;51:55–63. https://doi.org/10.1016/0014-4835(90)90170-Y.
21. Lütjen-Drecoll E, Tektas OY. In: Dartt DA, editor. Encyclopedia of the eye. New York: Academic Press; 2010. p. 224–8.
22. Tektas O-Y, Lütjen-Drecoll E. Structural changes of the trabecular meshwork in different kinds of glaucoma. Exp Eye Res. 2009;88:769–75. https://doi.org/10.1016/j.exer.2008.11.025.
23. Toris CB, Yablonski ME, Wang Y-L, Camras CB. Aqueous humor dynamics in the aging human eye. Am J Ophthalmol. 1999;127:407–12.
24. Toris CB, Koepsell SA, Yablonski ME, Camras CB. Aqueous humor dynamics in ocular hypertensive patients. J Glaucoma. 2002;11:253–8.
25. Johnson M, Shapiro A, Ethier CR, Kamm RD. Modulation of outflow resistance by the pores of the inner wall endothelium. Invest Ophthalmol Vis Sci. 1992;33:1670–5.
26. Janmey PA, McCulloch CA. Cell mechanics: integrating cell responses to mechanical stimuli. Annu Rev Biomed Eng. 2007;9:1–34. https://doi.org/10.1146/annurev.bioeng.9.060906.151927.
27. Mendez MG, Janmey PA. Transcription factor regulation by mechanical stress. Int J Biochem Cell Biol. 2012;44:728–32. https://doi.org/10.1016/j.biocel.2012.02.003.
28. Discher DE, Janmey P, Wang YL. Tissue cells feel and respond to the stiffness of their substrate. Science. 2005;310:1139–43. https://doi.org/10.1126/science.1116995.
29. Janmey PA, Wells RG, Assoian RK, McCulloch CA. From tissue mechanics to transcription factors. Differentiation. 2013;86:112–20. https://doi.org/10.1016/j.diff.2013.07.004.
30. Engler A, et al. Substrate compliance versus ligand density in cell on gel responses. Biophys J. 2004;86:617–28. https://doi.org/10.1016/S0006-3495(04)74140-5.
31. Engler AJ, Rehfeldt F, Sen S, Discher DE. In: Yu-Li W, Dennis ED, editors. Methods in cell biology, vol. 83. New York: Academic Press; 2007. p. 521–45.
32. Engler AJ, Sen S, Sweeney HL, Discher DE. Matrix elasticity directs stem cell lineage specification. Cell. 2006;126:677–89. https://doi.org/10.1016/j.cell.2006.06.044.
33. Califano JP, Reinhart-King CA. The effects of substrate elasticity on endothelial cell network formation and traction force generation. Conf Proc IEEE Eng Med Biol Soc. 2009;2009:3343–5. https://doi.org/10.1109/iembs.2009.5333194.
34. Califano JP, Reinhart-King CA. Substrate stiffness and cell area predict cellular traction stresses in single cells and cells in contact. Cell Mol Bioeng. 2010;3:68–75. https://doi.org/10.1007/s12195-010-0102-6.
35. Casey MK-R, Shawn PC, Joseph PC, Brooke NS, Cynthia AR-K. The role of the cytoskeleton in cellular force generation in 2D and 3D environments. Phys Biol. 2011;8:015009.
36. Kraning-Rush CM, Carey SP, Califano JP, Reinhart-King CA. Quantifying traction stresses in adherent cells. Methods Cell Biol. 2012;110:139–78. https://doi.org/10.1016/b978-0-12-388403-9.00006-0.
37. Lepple-Wienhues A, Stahl F, Wiederholt M. Differential smooth muscle-like contractile properties of trabecular meshwork and ciliary muscle. Exp Eye Res. 1991;53:33–8. https://doi.org/10.1016/0014-4835(91)90141-Z.
38. Wiederholt M, Lepple-Wienhues A, Stahl E. Electrical properties and contractility of the trabecular meshwork. Exp Eye Res. 1992;55(Suppl 1):41. https://doi.org/10.1016/0014-4835(92)90345-S.
39. Fuchshofer R, Tamm ER. In: Dartt DA, editor. Encyclopedia of the eye. New York: Academic Press; 2010. p. 28–36.
40. Tamm ER, Braunger BM, Fuchshofer R. In: Hejtmancik JF, John MN, editors. Progress in molecular biology and translational science, vol. 134. New York: Academic Press; 2015. p. 301–14.
41. Braunger BM, Fuchshofer R, Tamm ER. The aqueous humor outflow pathways in glaucoma: a unifying concept of disease mechanisms and causative treatment. Eur J. Pharm Biopharm. 2015;95:173–81. https://doi.org/10.1016/j.ejpb.2015.04.029.

42. Rao PV, Deng P, Sasaki Y, Epstein DL. Regulation of myosin light chain phosphorylation in the trabecular meshwork: role in aqueous humour outflow facility. Exp Eye Res. 2005;80:197–206. https://doi.org/10.1016/j.exer.2004.08.029.
43. Pattabiraman PP, Rao PV. Mechanistic basis of Rho GTPase-induced extracellular matrix synthesis in trabecular meshwork cells. Am J Physiol Cell Physiol. 2010;298:C749–63. https://doi.org/10.1152/ajpcell.00317.2009.
44. Ren R, et al. Netarsudil increases outflow facility in human eyes through multiple mechanisms. Invest Ophthalmol Vis Sci. 2016;57:6197–209. https://doi.org/10.1167/iovs.16-20189.
45. Overby DR, Stamer WD, Johnson M. The changing paradigm of outflow resistance generation: towards synergistic models of the JCT and inner wall endothelium. Exp Eye Res. 2009;88:656–70. https://doi.org/10.1016/j.exer.2008.11.033.
46. McDonnell F, Dismuke WM, Overby DR, Stamer WD. Pharmacological regulation of outflow resistance distal to Schlemm's Canal. Am J Physiol Cell Physiol. 2018; https://doi.org/10.1152/ajpcell.00024.2018.
47. Carreon TA, Edwards G, Wang H, Bhattacharya SK. Segmental outflow of aqueous humor in mouse and human. Exp Eye Res. 2017;158:59–66. https://doi.org/10.1016/j.exer.2016.08.001.
48. Cha EDK, Xu J, Gong L, Gong H. Variations in active outflow along the trabecular outflow pathway. Exp Eye Res. 2016;146:354–60. https://doi.org/10.1016/j.exer.2016.01.008.
49. de Kater AW, Melamed S, Epstein DL. Patterns of aqueous humor outflow in glaucomatous and nonglaucomatous human eyes. A tracer study using cationized ferritin. Arch Ophthalmol. 1989;107:572–6.
50. Hann CR, Bahler CK, Johnson DH. Cationic ferritin and segmental flow through the trabecular meshwork. Invest Ophthalmol Vis Sci. 2005;46:1–7. https://doi.org/10.1167/iovs.04-0800.
51. Swaminathan SS, Oh D-J, Kang MH, Rhee DJ. Aqueous outflow: segmental and distal flow. J Cataract Refract Surg. 2014;40:1263–72. https://doi.org/10.1016/j.jcrs.2014.06.020.
52. Vranka JA, Acott TS. Pressure-induced expression changes in segmental flow regions of the human trabecular meshwork. Exp Eye Res. 2016; https://doi.org/10.1016/j.exer.2016.06.009.
53. Vranka JA, et al. Biomechanical rigidity and quantitative proteomics analysis of segmental regions of the trabecular meshwork at physiologic and elevated pressures. Invest Ophthalmol Vis Sci. 2018;59:246–59. https://doi.org/10.1167/iovs.17-22759.
54. Johnstone MA. The aqueous outflow system as a mechanical pump - evidence from examination of tissue and aqueous movement in human and non-human primates. J Glaucoma. 2004;13:421–38. https://doi.org/10.1097/01.ijg.0000131757.63542.24.
55. Li P, Shen TT, Johnstone M, Wang RK. Pulsatile motion of the trabecular meshwork in healthy human subjects quantified by phase-sensitive optical coherence tomography. Biomed Opt Express. 2013;4:2051–65. https://doi.org/10.1364/boe.4.002051.
56. Last JA, et al. Elastic modulus determination of normal and glaucomatous human trabecular meshwork. Invest Ophthalmol Vis Sci. 2011;52:2147–52. https://doi.org/10.1167/iovs.10-6342.
57. Raghunathan VK, et al. Glaucomatous cell derived matrices differentially modulate nonglaucomatous trabecular meshwork cellular behavior. Acta Biomater. 2018;71:444–59. https://doi.org/10.1016/j.actbio.2018.02.037.
58. Morgan JT, Raghunathan VK, Thomasy SM, Murphy CJ, Russell P. Robust and artifact-free mounting of tissue samples for atomic force microscopy. BioTechniques. 2014;56:40–2. https://doi.org/10.2144/000114126.
59. Wang K, et al. Estimating human trabecular meshwork stiffness by numerical modeling and advanced OCT imaging. Invest Ophthalmol Vis Sci. 2017;58:4809–17. https://doi.org/10.1167/iovs.17-22175.
60. Camras LJ, Stamer WD, Epstein D, Gonzalez P, Yuan F. Differential effects of trabecular meshwork stiffness on outflow facility in normal human and porcine eyes. Invest Ophthalmol Vis Sci. 2012;53:5242–50. https://doi.org/10.1167/iovs.12-9825.
61. Camras LJ, Stamer WD, Epstein D, Gonzalez P, Yuan F. Circumferential tensile stiffness of glaucomatous trabecular meshwork. Invest Ophthalmol Vis Sci. 2014;55:814–23. https://doi.org/10.1167/iovs.13-13091.

62. Camras LJ, Stamer WD, Epstein D, Gonzalez P, Yuan F. Erratum. Invest Ophthalmol Vis Sci. 2014;55:2316. https://doi.org/10.1167/iovs.12-9825a.
63. Chang JY, Folz SJ, Laryea SN, Overby DR. Multi-scale analysis of segmental outflow patterns in human trabecular meshwork with changing intraocular pressure. J Ocul Pharmacol Ther. 2014;30:213–23. https://doi.org/10.1089/jop.2013.0182.
64. Keller KE, Bradley JM, Vranka JA, Acott TS. Segmental versican expression in the trabecular meshwork and involvement in outflow facility. Invest Ophthalmol Vis Sci. 2011;52:5049–57. https://doi.org/10.1167/iovs.10-6948.
65. Overby DR. The role of segmental outflow in the trabecular meshwork. ARVO SIG, e-SIG # 1221, 2010.
66. Stamer WD, Acott TS. Current understanding of conventional outflow dysfunction in glaucoma. Curr Opin Ophthalmol. 2012;23:135–43. https://doi.org/10.1097/ICU.0b013e32834ff23e.
67. Hatami-Marbini H, Etebu E. Hydration dependent biomechanical properties of the corneal stroma. Exp Eye Res. 2013;116:47–54. https://doi.org/10.1016/j.exer.2013.07.016.
68. Hatami-Marbini H, Rahimi A. Effects of bathing solution on tensile properties of the cornea. Exp Eye Res. 2014; https://doi.org/10.1016/j.exer.2013.11.017.
69. Hatami-Marbini H, Rahimi A. Evaluation of hydration effects on tensile properties of bovine corneas. J Cataract Refract Surg. 2015;41:644–51. https://doi.org/10.1016/j.jcrs.2014.07.029.
70. Hatami-Marbini H, Rahimi A. The relation between hydration and mechanical behavior of bovine cornea in tension. J Mech Behav Biomed Mater. 2014;36:90–7. https://doi.org/10.1016/j.jmbbm.2014.03.011.
71. Johnson M, Schuman JS, Kagemann L. Trabecular meshwork stiffness in the living human eye. Invest Ophthalmol Vis Sci. 2015;56:3541.
72. Pant AD, Kagemann L, Schuman JS, Sigal IA, Amini R. An imaged-based inverse finite element method to determine in-vivo mechanical properties of the human trabecular meshwork. J Model Ophthalmol. 2017;1:100–11.
73. Stewart WC, Magrath GN, Demos CM, Nelson LA, Stewart JA. Predictive value of the efficacy of glaucoma medications in animal models: preclinical to regulatory studies. Br J Ophthalmol. 2011;95:1355–60. https://doi.org/10.1136/bjo.2010.188508.
74. Johnstone MA, Grant WM. Pressure-dependent changes in structures of the aqueous outflow system of human and monkey eyes. Am J Ophthalmol. 1973;75:365–83.
75. Zhang Y, Toris CB, Liu Y, Ye W, Gong H. Morphological and hydrodynamic correlates in monkey eyes with laser induced glaucoma. Exp Eye Res. 2009;89:748–56. https://doi.org/10.1016/j.exer.2009.06.015.
76. Melamed S, Epstein DL. Alterations of aqueous humour outflow following argon laser trabeculoplasty in monkeys. Br J Ophthalmol. 1987;71:776–81.
77. Melamed S, Pei J, Epstein DL. Delayed response to argon laser trabeculoplasty in monkeys. Morphological and morphometric analysis. Arch Ophthalmol. 1986;104:1078–83.
78. Koss MC, March WF, Nordquist RE, Gherezghiher T. Acute intraocular pressure elevation produced by argon laser trabeculoplasty in the cynomolgus monkey. Arch Ophthalmol. 1984;102:1699–703.
79. Harwerth RS, et al. Visual field defects and neural losses from experimental glaucoma. Prog Retin Eye Res. 2002;21:91–125.
80. Raghunathan V, et al. Biomechanical, ultrastructural, and electrophysiological characterization of the non-human primate experimental glaucoma model. Sci Rep. 2017;7:14329. https://doi.org/10.1038/s41598-017-14720-2.
81. Li G, et al. Disease progression in iridocorneal angle tissues of BMP2-induced ocular hypertensive mice with optical coherence tomography. Mol Vis. 2014;20:1695–709.
82. Wang K, Read AT, Sulchek T, Ethier CR. Trabecular meshwork stiffness in glaucoma. Exp Eye Res. 2017;158:3–12. https://doi.org/10.1016/j.exer.2016.07.011.
83. Wang K, et al. The relationship between outflow resistance and trabecular meshwork stiffness in mice. Sci Rep. 2018;8:5848. https://doi.org/10.1038/s41598-018-24165-w.

84. Whitlock NA, McKnight B, Corcoran KN, Rodriguez LA, Rice DS. Increased intraocular pressure in mice treated with dexamethasone. Invest Ophthalmol Vis Sci. 2010;51:6496–503. https://doi.org/10.1167/iovs.10-5430.
85. Weinreb RN, Polansky JR, Kramer SG, Baxter JD. Acute effects of dexamethasone on intraocular pressure in glaucoma. Invest Ophthalmol Vis Sci. 1985;26:170–5.
86. Huang J, Camras LJ, Yuan F. Mechanical analysis of rat trabecular meshwork. Soft Matter. 2015; https://doi.org/10.1039/c4sm01949k.
87. Yuan F, Camras LJ, Gonzalez P. Trabecular meshwork stiffness in ex vivo perfused porcine eyes. Invest Ophthalmol Vis Sci. 2011;52:6693.
88. Ebenstein DM, Pruitt LA. Nanoindentation of biological materials. Nano Tod. 2006;1:26–33. https://doi.org/10.1016/S1748-0132(06)70077-9.
89. Oyen ML. Nanoindentation of biological and biomimetic materials. Exp Tech. 2013;37:73–87. https://doi.org/10.1111/j.1747-1567.2011.00716.x.
90. Dias JM, Ziebarth NM. Anterior and posterior corneal stroma elasticity assessed using nanoindentation. Exp Eye Res. 2013;115:41–6. https://doi.org/10.1016/j.exer.2013.06.004.
91. Harding J, Sneddon I. The elastic stresses produced by the indentation of the plane surface of a semi-infinite elastic solid by a rigid punch. Cambridge: Cambridge University Press; 2008. p. 16–26.
92. Love AEH. Boussingesq's problem for a rigid cone. Q J Math. 1939;10:161–75.
93. Cheng L, Xia X, Scriven LE, Gerberich WW. Spherical-tip indentation of viscoelastic material. Mech Mater. 2005;37:213–26. https://doi.org/10.1016/j.mechmat.2004.03.002.
94. Cheng Y-T, Cheng C-M. Relationships between initial unloading slope, contact depth, and mechanical properties for spherical indentation in linear viscoelastic solids. Mater Sci Eng A. 2005;409:93–9. https://doi.org/10.1016/j.msea.2005.05.118.
95. Rodriguez ML, McGarry PJ, Sniadecki NJ. Review on cell mechanics: experimental and modeling approaches. Appl Mech Rev. 2013;65:060801. https://doi.org/10.1115/1.4025355.
96. Rodríguez R, Gutierrez I. Correlation between nanoindentation and tensile properties: influence of the indentation size effect. Mater Sci Eng A. 2003;361:377–84. https://doi.org/10.1016/S0921-5093(03)00563-X.
97. Oliver WC, Pharr GM. Improved technique for determining hardness and elastic modulus using load and displacement sensing indentation experiments. J Mater Res. 1992;7:1564–83.
98. Pharr G, Oliver W, Brotzen F. On the generality of the relationship among contact stiffness, contact area, and elastic modulus during indentation. J Mater Res. 1992;7:613–7.
99. Gasiorowski JZ, Murphy CJ, Nealey PF. Biophysical cues and cell behavior: the big impact of little things. Annu Rev Biomed Eng. 2013;15:155–76. https://doi.org/10.1146/annurev-bioeng-071811-150021.
100. Gasiorowski JZ, Russell P. Biological properties of trabecular meshwork cells. Exp Eye Res. 2009;88:671–5. https://doi.org/10.1016/j.exer.2008.08.006.
101. Schlunck G, et al. Substrate rigidity modulates cell–matrix interactions and protein expression in human trabecular meshwork cells. Invest Ophthalmol Vis Sci. 2008;49:262–9. https://doi.org/10.1167/iovs.07-0956.
102. Han H, Wecker T, Grehn F, Schlunck G. Elasticity-dependent modulation of TGF-β responses in human trabecular meshwork cells. Invest Ophthalmol Vis Sci. 2011;52:2889–96.
103. Morgan JT, Murphy CJ, Russell P. What do mechanotransduction, Hippo, Wnt, and TGFbeta have in common? YAP and TAZ as key orchestrating molecules in ocular health and disease. Exp Eye Res. 2013;115:1–12. https://doi.org/10.1016/j.exer.2013.06.012.
104. Raghunathan VK, et al. Role of substratum stiffness in modulating genes associated with extracellular matrix and mechanotransducers YAP and TAZ. Invest Ophthalmol Vis Sci. 2012;54:378–86.
105. Babizhayev MA, Yegorov YE. Senescent phenotype of trabecular meshwork cells displays biomarkers in primary open-angle glaucoma. Curr Mol Med. 2011;11:528–52.

106. Morgan JT, Raghunathan VK, Chang Y-R, Murphy CJ, Russell P. Wnt inhibition induces persistent increases in intrinsic stiffness of human trabecular meshwork cells. Exp Eye Res. 2015;132:174–8.
107. Morgan JT, Raghunathan VK, Chang Y-R, Murphy CJ, Russell P. The intrinsic stiffness of human trabecular meshwork cells increases with senescence. Oncotarget. 2015; https://doi.org/10.18632/oncotarget.3798.
108. Raghunathan VK, et al. Dexamethasone stiffens trabecular meshwork, trabecular meshwork cells, and matrix. Invest Ophthalmol Vis Sci. 2015;56:4447–59. https://doi.org/10.1167/iovs.15-16739.
109. Wood JA, et al. Substratum compliance regulates human trabecular meshwork cell behaviors and response to latrunculin B. Invest Ophthalmol Vis Sci. 2011;52:9298–303. https://doi.org/10.1167/iovs.11-7857.
110. Thomasy SM, Wood JA, Kass PH, Murphy CJ, Russell P. Substratum stiffness and latrunculin B regulate matrix gene and protein expression in human trabecular meshwork cells. Invest Ophthalmol Vis Sci. 2012;53:952–8. https://doi.org/10.1167/iovs.11-8526.
111. Thomasy SM, Morgan JT, Wood JA, Murphy CJ, Russell P. Substratum stiffness and latrunculin B modulate the gene expression of the mechanotransducers YAP and TAZ in human trabecular meshwork cells. Exp Eye Res. 2013;113:66–73. https://doi.org/10.1016/j.exer.2013.05.014.
112. McKee CT, et al. The effect of biophysical attributes of the ocular trabecular meshwork associated with glaucoma on the cell response to therapeutic agents. Biomaterials. 2011;32:2417–23. https://doi.org/10.1016/j.biomaterials.2010.11.071.
113. Russell P, Gasiorowski JZ, Nealy PF, Murphy CJ. Response of human trabecular meshwork cells to topographic cues on the nanoscale level. Invest Ophthalmol Vis Sci. 2008;49:629–35. https://doi.org/10.1167/iovs.07-1192.
114. Baetz NW, Hoffman EA, Yool AJ, Stamer WD. Role of aquaporin-1 in trabecular meshwork cell homeostasis during mechanical strain. Exp Eye Res. 2009;89:95–100. https://doi.org/10.1016/j.exer.2009.02.018.
115. Liton PB, et al. Induction of IL-6 expression by mechanical stress in the trabecular meshwork. Biochem Biophys Res Commun. 2005;337:1229–36. https://doi.org/10.1016/j.bbrc.2005.09.182.
116. Porter KM, Jeyabalan N, Liton PB. MTOR-independent induction of autophagy in trabecular meshwork cells subjected to biaxial stretch. Biochim Biophys Acta. 2014;1843:1054–62. https://doi.org/10.1016/j.bbamcr.2014.02.010.
117. Okada Y, Matsuo T, Ohtsuki H. Bovine trabecular cells produce TIMP-1 and MMP-2 in response to mechanical stretching. Jpn J Ophthalmol. 1998;42:90–4. https://doi.org/10.1016/S0021-5155(97)00129-9.
118. Wu J, et al. Endogenous production of extracellular adenosine by trabecular meshwork cells: potential role in outflow regulation. Invest Ophthalmol Vis Sci. 2012;53:7142–8. https://doi.org/10.1167/iovs.12-9968.
119. Luna C, et al. Extracellular release of ATP mediated by cyclic mechanical stress leads to mobilization of AA in trabecular meshwork cells. Invest Ophthalmol Vis Sci. 2009;50:5805–10. https://doi.org/10.1167/iovs.09-3796.
120. Maddala R, Skiba NP, Rao PV. Vertebrate lonesome kinase regulated extracellular matrix protein phosphorylation, cell shape, and adhesion in trabecular meshwork cells. J Cell Physiol. 2017;232:2447–60. https://doi.org/10.1002/jcp.25582.
121. Iyer P, et al. Autotaxin-lysophosphatidic acid axis is a novel molecular target for lowering intraocular pressure. PLoS One. 2012;7:e42627. https://doi.org/10.1371/journal.pone.0042627.
122. Mitton KP, et al. Transient Loss of αB-crystallin: an early cellular response to mechanical stretch. Biochem Biophys Res Commun. 1997;235:69–73. https://doi.org/10.1006/bbrc.1997.6737.

123. Tumminia SJ, et al. Mechanical stretch alters the actin cytoskeletal network and signal transduction in human trabecular meshwork cells. Invest Ophthalmol Vis Sci. 1998;39:1361–71.
124. WuDunn D. The effect of mechanical strain on matrix metalloproteinase production by bovine trabecular meshwork cells. Curr Eye Res. 2001;22:394–7.
125. Bradley JM, et al. Effects of mechanical stretching on trabecular matrix metalloproteinases. Invest Ophthalmol Vis Sci. 2001;42:1505–13.
126. Bradley JM, Kelley MJ, Rose A, Acott TS. Signaling pathways used in trabecular matrix metalloproteinase response to mechanical stretch. Invest Ophthalmol Vis Sci. 2003;44:5174–81.
127. Raghunathan VK, et al. Transforming growth factor Beta 3 modifies mechanics and composition of extracellular matrix deposited by human trabecular meshwork cells. ACS Biomater Sci Eng. 2015;1:110–8. https://doi.org/10.1021/ab500060r.
128. Torrejon KY, et al. Recreating a human trabecular meshwork outflow system on microfabricated porous structures. Biotechnol Bioeng. 2013;110:3205–18. https://doi.org/10.1002/bit.24977.
129. Torrejon KY, et al. TGFβ2-induced outflow alterations in a bioengineered trabecular meshwork are offset by a rho-associated kinase inhibitor. Sci Rep. 2016;6:38319. https://doi.org/10.1038/srep38319.
130. Chu ER, Gonzalez JM, Tan JCH. Tissue-based imaging model of human trabecular meshwork. J Ocul Pharmacol Ther. 2014;30:191–201. https://doi.org/10.1089/jop.2013.0190.
131. Gonzalez JM, Hamm-Alvarez S, Tan JCH. Analyzing live cellularity in the human trabecular meshwork. Invest Ophthalmol Vis Sci. 2013;54:1039–47. https://doi.org/10.1167/iovs.12-10479.
132. Gonzalez JM, Heur M, Tan JCH. Two-photon immunofluorescence characterization of the trabecular meshwork in situ. Invest Ophthalmol Vis Sci. 2012;53:3395–404. https://doi.org/10.1167/iovs.11-8570.